# AMSR-E/AMSR2 Unified L2B Global Swath Surface Precipitation, Version 1

## USER GUIDE

**How to Cite These Data**

As a condition of using these data, you must include a citation:

Kummerow, C., R. Ferraro, and D. Randel. 2020. *AMSR-E/AMSR2 Unified L2B Global Swath Surface Precipitation, Version 1*. [Indicate subset used]. Boulder, Colorado USA. NASA National Snow and Ice Data Center Distributed Active Archive Center. https://doi.org/10.5067/P5MCTDH7674A. [Date Accessed].

FOR QUESTIONS ABOUT THESE DATA, CONTACT NSIDC@NSIDC.ORG

FOR CURRENT INFORMATION, VISIT https://nsidc.org/data/AU_Rain

National Snow and Ice Data Center

# TABLE OF CONTENTS



# 1 DATA DESCRIPTION

This data set contains instantaneous surface precipitation rates and types over land and ocean, and precipitation profiles over ocean. The data are derived from observations acquired by the Advanced Microwave Scanning Radiometer (AMSR) for EOS (AMSR-E) and AMSR2 instruments, using a common (i.e., “unified”) algorithm.

## 1.1 Parameters

Parameters are listed and described in Table 1 and Table 2.

Table 1. Parameter Descriptions

| Parameter | Description | Units | Fill Value |
|---|---|---|---|
| CloudWaterPath | Total cloud liquid water in atmospheric column | $kg/m^2$ | -9999.0 |
| RainWaterPath | Total rainwater in atmospheric column | $kg/m^2$ | -9999.0 |
| IceWaterPath | Total cloud ice in atmospheric column | $kg/m^2$ | -9999.0 |
| ConvectivePrecip | Instantaneous convective precipitation rate | mm/hr | -9999.0 |
| FrozenPrecip | Instantaneous frozen precipitation rate | mm/hr | -9999.0 |
| SurfacePrecip | Instantaneous total precipitation rate | mm/hr | -9999.0 |
| Temp2Meter* | Temperature at 2 m (T2m) in Kelvin | K | -999 |
| TotalColWaterVapor | Integrated water vapor in atmospheric column (TCWV). Synonymous with Total Precipitable Water (TPW). | mm | -99 |
| L1RQualFlag | Reserved for future use (set to 0) | n/a | -99 |
| SunglintAngle | Angle between reflected sunlight and AMSR2 line of sight | degree | -88 |
| ProbabilityofPrecip | Likelihood of precipitation, defined as the fraction of precipitation vs non-precipitation database profiles in the output solution (provided due to the nature of the precipitation retrieval). | percent | -99 |
| QualityFlag | Retrieval quality (See “Section 2.5.5 \| Quality Flags”):<br>0: Good<br>1: Use with caution<br>2: Use pixel with extreme care over snow covered surface<br>3: Use with extreme caution | n/a | -99 |

| Parameter | Description | Units | Fill Value |
|---|---|---|---|
| PixelStatus | Quality indicator for the pixel. Non-valid pixels (1 - 5) cause the algorithm to fail due to:<br>0: Valid Pixel<br>1: Invalid geolocation<br>2: Sensor brightness temperatures out of range<br>3: Surface code histogram mismatch<br>4: Missing TCWV, T2m or sfccode (surface code)<br>5: No Bayesian solution for pixel | n/a | -99 |
| SurfaceTypeIndex* | Surface type, classified as:<br>1: Ocean<br>2: Sea-ice<br>3-7: Decreasing vegetation coverage (3 = max, 7 = min)<br>8-11: Decreasing snow coverage (8 = max, 11 = min)<br>12: Inland water<br>13: Land/water boundary - coast<br>14: Sea-ice ocean boundary | n/a | -99 |

*Input/pass-through parameter to the AMSR Unified Rainfall algorithm.

Table 2. Geolocation Parameters

| Parameter | Description | Units | Fill Value |
|---|---|---|---|
| Latitude | Latitude, center of pixel | °N | -9999.0 |
| Longitude | Longitude, center of pixel | °E | -9999.0 |
| SCalt | Spacecraft altitude | km | -9999.0 |
| SClat | Spacecraft latitude | °N | -9999.0 |
| SClon | Spacecraft longitude | °E | -9999.0 |
| scantime | Scan time along track in year, month, day, hour, minute and second | n/a | n/a |
| tai93time | Scan time along track measured in seconds since 1993-01-01 00:00:00 | seconds | -9999.0 |

## 1.2 Sample Data Image

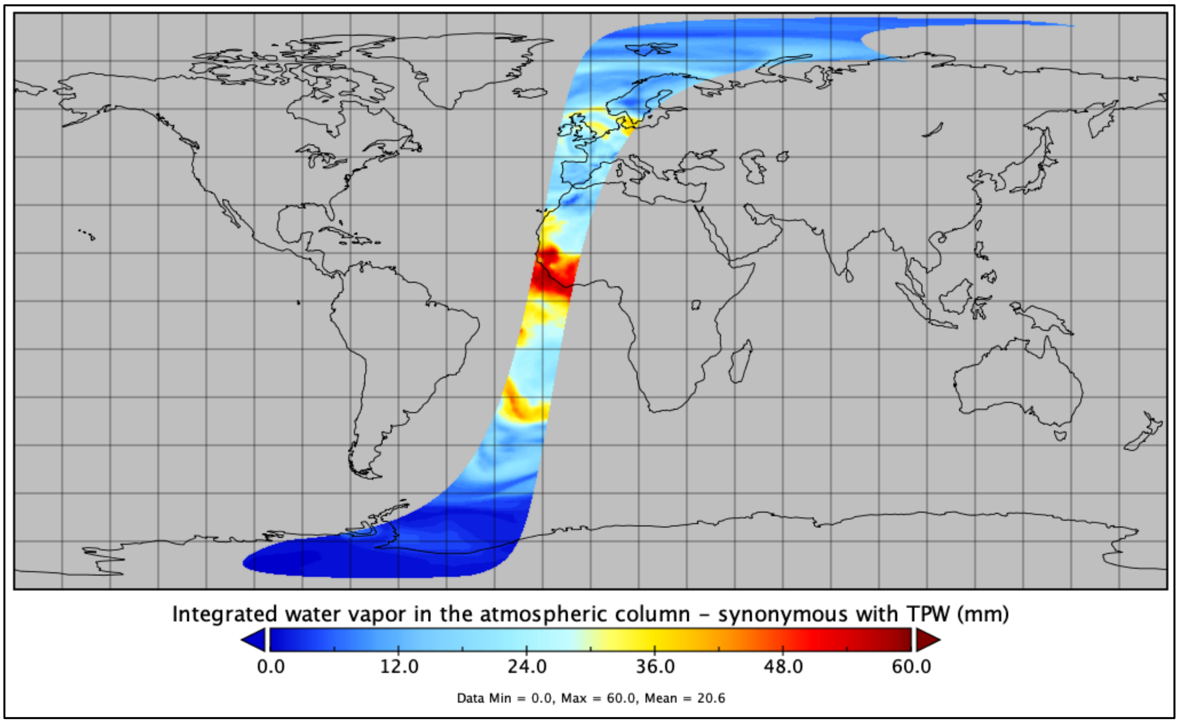


Figure 1. Total Column Water Vapor, 13 June 2020 (AMSR2)

## 1.3 File Information

### 1.3.1 Format

Data are provided in HDF-EOS5 format files. In addition, corresponding product history, quality assurance, and science metadata files are available for each data file. Approximately 30 data files are generated each day, one for each ascending and descending half orbit.

### 1.3.2 File Contents

Data files are organized into groups. Science and geolocation parameters are stored in the "SWATHS/[sensor]/Data_Fields" and "SWATHS/[sensor]/Geolocation_Fields" groups, respectively. HDF-EOS global attributes are stored in "HDFEOS_INFORMATION."

The following figure shows the structure of an AU_Rain data file of AMSR2 observations:

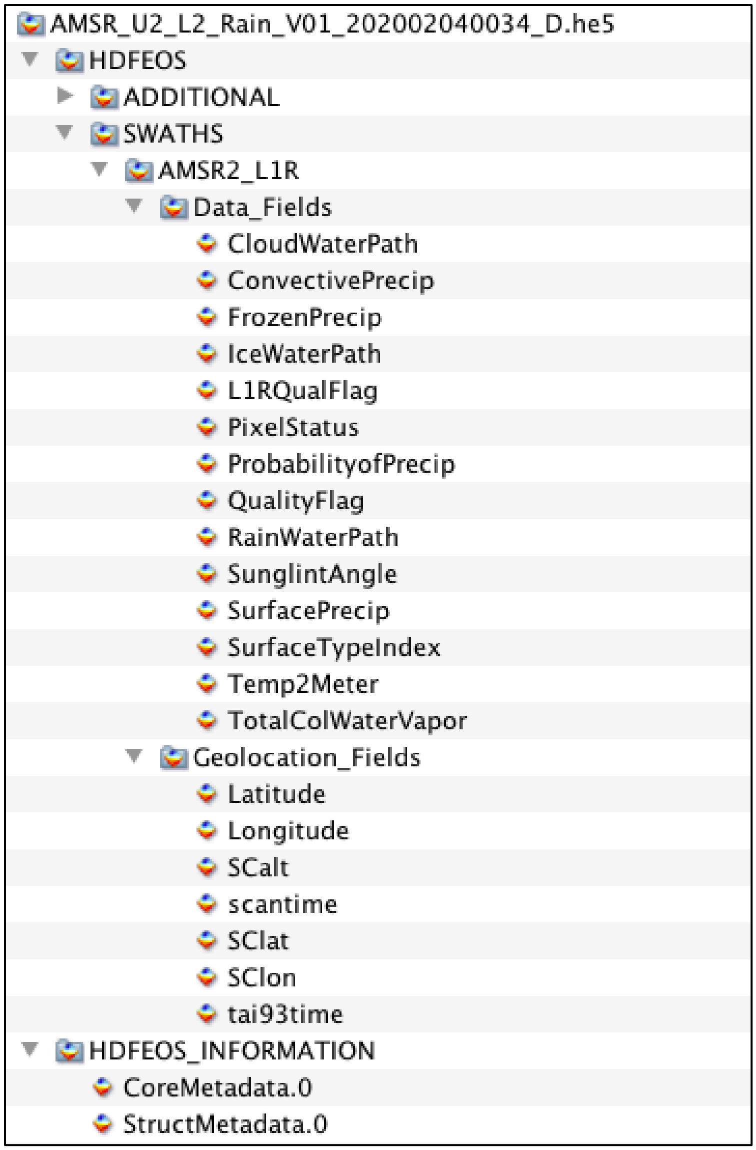


Figure 2. AU_Rain Data File of AMSR2 Observations

## 1.3.3 Naming Convention

Files are named according to the following convention and as described in Tables 3, 4, and 5.

**Example File Names**

AMSR_U2_L2_Rain_V01_201909010009_D.he5

AMSR_UE_L2_Rain_V02_200601010002_A.he5

**Naming Convention**

AMSR_U[*sensor*]_L2_Rain_[*maturity code*][*iteration number*]_[*date*][*time*]_[*direction*].[*ext*]

Table 3. File Name Description

| Variable | Description |
|---|---|
| AMSR_U | Advanced Microwave Sounding Radiometer Unified |
| sensor | 2 = AMSR2, E = AMSR-E |
| L2 | Data Processing Level 2 |
| Rain | Product identifier (i.e., precipitation product) |
| maturity code | Product maturity letter code: P, B, T, or V (see Table 4) |
| iteration number | File iteration number (see Table 5) |
| date | Four-digit year, two-digit month, two-digit day. E.g., 20190901 = 01 November 2019 |
| time | Two-digit hour, two-digit minute (24h, UTC) of first scan in the file. E.g., 0009 = 00:09 (UTC) |
| direction | Orbit direction. A = ascending, D = descending |
| ext | File extension. he5 = HDF-EOS5; .qa = quality assurance; ph = product history; xml = science metadata |

### 1.3.3.1 Maturity Code

Maturity codes indicate which version of the algorithm was used to produce the data, using a letter (see Table 4) and a two-digit iteration number (see Table 5).

Table 4. Product Maturity Code Descriptions

| Variable | Description |
|---|---|
| P | Preliminary - refers to non-standard, near-real-time data available from the NSIDC DAAC. These data are only available for a limited time until the corresponding standard product is ingested at the NSIDC DAAC. |
| B | Beta - indicates a developing algorithm with updates anticipated. |
| T | Transitional - period between beta and validated, where the product has passed the beta stage but is not quite ready to be validated. This is where the algorithm matures and stabilizes. |
| V | Validated - products are upgraded to validated once the algorithm is verified by the algorithm team and validated by the validation teams. As shown in Table 5, validated products also have an associated validation stage. |

Table 5. Validation Stage Descriptions

| Validation Stage | Description |
|---|---|
| Stage 1 | Product accuracy is estimated using a small number of independent measurements obtained from selected locations, time periods, and ground-truth/field program efforts. |
| Stage 2 | Product accuracy is assessed over a widely distributed set of locations and time periods via several ground-truth and validation efforts. |
| Stage 3 | Product accuracy is assessed, and the uncertainties in the product are well established via independent measurements made in a systematic and statistically robust way that represents global conditions. |

## 1.4 Spatial Information

### 1.4.1 Coverage

Coverage extends from 89°24' N to 89°24' S. Figure 3 shows the typical spatial coverage for a single day.

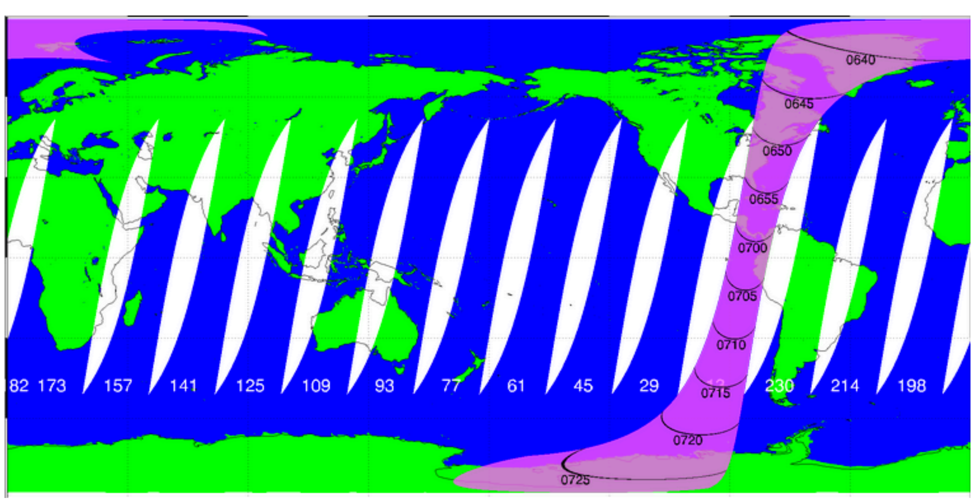

Figure 3. This map shows the AMSR2 half-orbit, descending pass (purple) for path 13D on 21 April 2020. The numbers (white) listed across the image indicate descending orbit paths.

### 1.4.2 Resolution

The pixel spacing is 10 km along track and 5 km along scan. However, the effective resolution is defined by the field of view (FOV), which varies with frequency for the AMSR instruments. Studies of the derived rainfall distribution indicate that the effective resolution is similar to the 22 GHz channel: 26 km along track and 15 km along scan.

## 1.5 Temporal Information

1 June 2002 to 4 October 2011

2 July 2012 to present

**Note:** Data are not available between 04 October 2011 – 02 July 2012, i.e., the end of the AMSR-E mission and the beginning of AMSR2.

### 1.5.1 Resolution

Each half-orbit swath spans approximately 50 minutes.

# 2 DATA ACQUISITION AND PROCESSING

## 2.1 Background

The AMSR Unified Rainfall algorithm uses intercalibrated, L1R brightness temperatures from AMSR-E and AMSR2 to create a consistent precipitation data record from the two satellites. The passive microwave algorithm is designed to take advantage of previously constructed, a priori databases of observed precipitation structures and their associated brightness temperatures, acquired by the Global Precipitation Measurement (GPM) mission. These databases are used in conjunction with Bayesian inversion techniques to retrieve surface precipitation and integrated liquid and ice-water contents.

The main algorithm output includes atmospheric profiles (path parameters) and surface precipitation rates. The path parameters are calculated for pixels over ocean only and provide the total amount of cloud water, rainwater, and ice-water included in the atmospheric column. The surface precipitation parameters are calculated for both ocean and land pixels and provide the instantaneous surface precipitation rate for convective precipitation, frozen precipitation, and total precipitation.

## 2.2 Acquisition

The AMSR-E insturment was a 12 channel, six frequency passive-microwave radiometer system. It measured horizontally and vertically polarized brightness temperatures at 6.9 GHz, 10.7 GHz, 18.7 GHz, 23.8 GHz, 36.5 GHz, and 89.0 GHz (the 6.9 GHz channel is not used for precipitation).

The AMSR2 instrument is a 7 frequency, total-power passive microwave radiometer system that measures horizontally and vertically polarized brightness temperatures at 6.925 GHz, 7.3 GHz, 10.65 GHz, 18.7 GHz, 23.8 GHz, 36.5 GHz, and 89.0 GHz (the 6.925 GHz and the 7.3 GHz channels are not used for precipitation).

The AMSR-E footprint size of each frequency can differ by several tens of kilometers. In addition, the center of a footprint at each frequency that corresponds to the same pixel and scan numbers can differ within a range of several kilometers, owing to the difference in the locations of the horns of the main rotating reflector. As such, the brightness temperatures at each frequency, despite being stored in the same pixel and scan numbers of the L1B product, may have been measured in different locations. AMSR2 uses a similar measurement mechanism to AMSR-E and experiences a decline in the footprint size and center at different frequencies.

To compensate, some footprints (antenna patterns) in the L1R products are convolved to obtain weighting factors relative to the 89.0 GHz channel, which are applied to obtain corrected footprints. This procedure is detailed in the Level 1R documentation.

In addition to the L1R data, the ancillary products listed in Table 5 are input to the algorithm. Note that Temp2Meter, TotalColWaterVapor, and SurfaceType are included in the output parameters.

Table 6. Ancillary data included in the AMSR Unified Rainfall Algorithm

| Product | Source | Description |
|---|---|---|
| Temp2Meter | GEOS-5 FP-IT* | Near surface temperature (T2m) |
| TotalColWaterVapor | GEOS-5 FP-IT* | Total column water vapor |
| Snow/no-snow classification | GEOS-5 FP-IT* | Snow cover classification |
| Sea ice coverage | GEOS-5 FP-IT* | Sea ice cover |
| SurfaceType | Aires et al. (2011) | Goddard profiling algorithm static surface classes |
| *Global Modeling and Assimilation Office Forward Processing for Instrument Teams (Located at GSFC) | | |

## 2.3 Processing

The following section summarizes the approach used to generate the AU_Rain data product. For a more complete description, see the AMSR Unified Rainfall ATBD (Kummerow et al., 2016), the Goddard Profiling (GPROF) literature (Kummerow et al., 2015), and the Global Precipitation Measurement (GPM) Mission ATBD.

As mentioned above, the processing is designed to take advantage of previously constructed a priori databases of observed precipitation structures from the GPM mission. The profiles in the a priori databases are created by the GPM Radar/Radiometer 'Combined' algorithm over oceans and by the GPM Dual Frequency Radar (DPR) Ku-band Radar over land. However, an exception is made for snow-covered areas: in these cases, the precipitation profiles are created from ground-based, radar-derived snowfall rates, which are matched directly to $T_b$ observations to create the precipitation profile.

Radiative transfer calculations are then applied to GPM observed cloud and precipitation structures to generate a database of simulated $T_b$; AMSR-E/AMSR2 L1R $T_b$ observations are subsequently compared against the simulated $T_b$ to find the best match from which to obtain the estimated rainfall rate.

Once the profile database and corresponding simulated AMSR-E/AMSR2 $T_b$ are established, the AMSR Unified Rainfall algorithm uses a Bayesian inversion methodology to calculate the probability of observing a profile R for a particular AMSR-E/AMSR2 $T_b$ vector. As shown in Equation 1, this probability, Pr(R | $T_b$), is calculated as the product of two other probabilities: Pr(R), the probability of observing this particular profile for no particular $T_b$ vector; and Pr($T_b$ | R), the probability of observing the specified $T_b$ vector at the same profile, R:

Eq. 1: $$Pr(R|T_b) = \Pr(R) \times \Pr(T_b|R),$$

The first term on the right-hand side of Equation 1 is derived from the precipitation profiles (Kummerow et al., 2014); the second is obtained from radiative transfer computations using the cloud model profiles. The weighting of each model profile in the compositing procedure is based on an exponential factor containing the mean square difference of the sensor-observed $T_b$ and a corresponding set of $T_b$ obtained from radiative transfer calculations through the cloudy atmosphere represented by the model profile. In summary, the retrieval procedure composes a new hydrometeor profile by taking the weighted sum of structures in the cloud structure database that are radiometrically consistent with the observations. The formal solution to the above problem is presented in detail in Kummerow et al. (1996).

The profile retrieval method is an adaptation of the well-known minimum variance solution for obtaining an optimal estimate of geophysical parameters from available information (Lorenc, 1986). While the mechanics of Bayesian inversions are fairly well understood, the AMSRU code does not search the entire a priori database, but instead searches only a subset of profiles with coincident near-surface temperature (T2m) and Total Column Water Vapor (TCWV) within 16 distinct surface classes, as described by Prigent and Aires (2011). The surface database (shown in Figure 4) is static, except for the snow/no-snow classification and sea ice classification, which like T2m and TCWV, are provided by the Global Modeling and Assimilation Office Forward Processing for Instrument Teams (GEOS-5 FP-IT) at the Goddard Space Flight Center.

The algorithm runs in two steps because of the ancillary data requirements. The pre-processor first ingests the L1R and ancillary data and produces an intermediate file. The algorithm then reads the database profiles and computes the most likely precipitation rate.

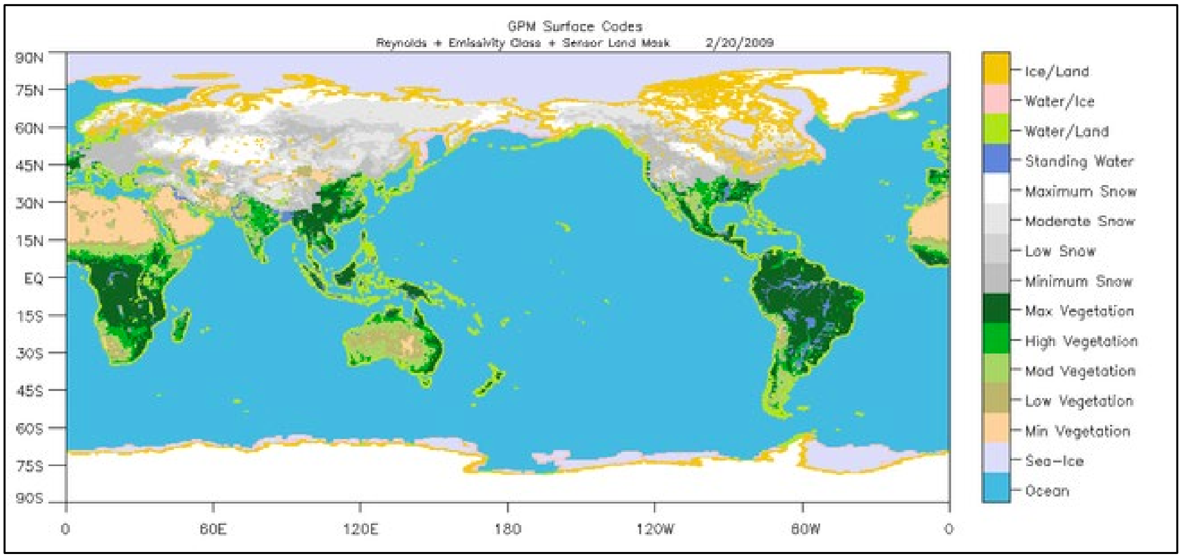


Figure 4. GPROF status surface classes. If GEOS5 FP-IT suggests that no snow is present in a snow-covered class, the most recent vegetated class for that pixel is used. Conversely, if snow is indicated by GEOS5 FP-IT in a vegetated class, then minimum snow is assigned to that pixel. Sea ice is assigned dynamically based on GEOS5 FP-IT.

## 2.4 Quality, Errors, and Limitations

### 2.4.1 Quality Information

Each HDF-EOS5 data file contains core metadata with Quality Assessment (QA) metadata flags that are set by the operational processing code run by the AMSR Science Investigator-led Processing System (SIPS). These QA flags are also provided in a separate XML metadata file.

### 2.4.2 Science QA

The processing code at the SIPS checks the maximum and minimum variable values and the percent of missing and out-of-bounds data per variable. Science QA also includes the following steps:

- Historical data comparisons
- Detection of errors in geolocation
- Verification of calibration data
- Trends in calibration data
- Detection of large scatter among data points that should be consistent

### 2.4.3 Quality Flags

The QualityFlag variable is included in the data file and provides a generalized quality retrieval measure for each pixel, with pixel values ranging from 0 to 3. Descriptions for each of the pixel values are provided below:

0. **Good**
   Highest confidence
1. **Use with caution**
   Pixels can be set to 1 for the following reasons: Sunglint is present, RFI, geolocate, warm load or for other L1R 'positive value' quality warning flags.
2. **Use with extreme care over snow-covered surface**
   Special value for snow-covered surfaces only. The pixel is set to 2 if the probability of precipitation is of poor quality or indeterminate. Use these pixels for climatological averaging of precipitation, but not for individual storm-scale daily cases.
3. **Use with extreme caution**
   Pixels are set to 3 if they have channels missing critical to the retrieval, but the choice has been made to continue the retrieval for the pixel.

## 2.5 Errors

Quantifying errors in this data set is complicated because it involves understanding the nature of precipitation. Uncertainties arise when the rain layer thickness is not well understood, or when inhomogeneous rainfall occurs below the resolution of the satellite. Another potential source of error is the non-precipitating component of clouds, which contribute to $T_b$. Scattering-based retrievals over land also present many uncertainties, most notably the lack of a consistent relationship between frozen rain aloft and liquid rain at lower altitudes. Quantifying the scattering by ice is especially problematic. Ambiguities occur in the data because microwave radiation is scattered not only by rainfall and associated ice but by snow cover and dry land (Kummerow and Ferraro, 2007).

## 2.6 Limitations

The following limitations have been identified:

- Shallow orographic precipitation remains a challenge for passive microwave sensors. Without an ice scattering signature, shallow warm rain, often associated with orographic precipitation, is difficult to distinguish from noise.
- High-latitude oceanic precipitation also remains a problem. GPM radars do not have enough sensitivity to detect light drizzle, and the AMSR instruments themselves have difficulties separating cloud water from drizzle. As such, the results are less certain in areas where much of the precipitation falls as drizzle.
- Light snowfall is also difficult to detect, as snow on the ground can look similar to light precipitating snow.

## 2.7 Instrumentation

AMSR-E was a modified version of the AMSR sensor that flew on the Japan Aerospace Exploration Agency (JAXA) Advanced Earth Observing Satellite-II (ADEOS-II). Developed in cooperation with U.S. and Japanese scientists, the AMSR-E instrument was provided to NASA by JAXA for the Aqua satellite. For more information about AMSR-E, see AMSRE-E Instrument Description.

AMSR2 was launched on May 18, 2012 on board the JAXA GCOM-W1 satellite. Additional information about the AMSR2 instrument is available on the GCOM-W1 | AMSR2 Channel Specification and Products page.

# 3 CONTACTS AND ACKNOWLEDGMENTS

**Christian D. Kummerow**
Colorado State University
Fort Collins, CO

**Ralph Ferraro**
CICS / University of Maryland
College Park, MD

**David Randel**
Colorado State University
Fort Collins, CO

# 4 REFERENCES

Aires, F., Prigent, C., Bernardo, F., Jiménez, C., Saunders, R., & Brunel, P. (2011). A Tool to Estimate Land-Surface Emissivities at Microwave frequencies (TELSEM) for use in numerical weather prediction. Quarterly Journal of the Royal Meteorological Society, 137(656), 690–699. https://doi.org/10.1002/qj.803

Conway, D. 2002. Advanced Microwave Scanning Radiometer - EOS Quality Assurance Plan. Huntsville, AL Global Hydrology and Climate Center.

Kummerow, C. D., Ringerud, S., Crook, J., Randel, D., & Berg, W. (2011). An Observationally Generated A Priori Database for Microwave Rainfall Retrievals. Journal of Atmospheric and Oceanic Technology, 28(2), 113–130. https://doi.org/10.1175/2010jtecha1468.1

Lorenc, A. C. (1986). Analysis methods for numerical weather prediction. Quarterly Journal of the Royal Meteorological Society, 112(474), 1177–1194. https://doi.org/10.1002/qj.49711247414

Reynolds, R. W., Smith, T. M., Liu, C., Chelton, D. B., Casey, K. S., & Schlax, M. G. (2007). Daily High-Resolution-Blended Analyses for Sea Surface Temperature. Journal of Climate, 20(22), 5473–5496. https://doi.org/10.1175/2007jcli1824.1

Kummerow, C. D., Randel, D. L., Kulie, M., Wang, N.-Y., Ferraro, R., Joseph Munchak, S., & Petkovic, V. (2015). The Evolution of the Goddard Profiling Algorithm to a Fully Parametric Scheme. Journal of Atmospheric and Oceanic Technology, 32(12), 2265–2280. https://doi.org/10.1175/jtech-d-15-0039.1

Hou, A. Y., Kakar, R. K., Neeck, S., Azarbarzin, A. A., Kummerow, C. D., Kojima, M., Oki, R., Nakamura, K., & Iguchi, T. (2014). The Global Precipitation Measurement Mission. Bulletin of the American Meteorological Society, 95(5), 701–722. https://doi.org/10.1175/bams-d-13-00164.1

Berg, W., L'Ecuyer, T., & Kummerow, C. (2006). Rainfall Climate Regimes: The Relationship of Regional TRMM Rainfall Biases to the Environment. Journal of Applied Meteorology and Climatology, 45(3), 434–454. https://doi.org/10.1175/jam2331.1

# 5 DOCUMENT INFORMATION

## 5.1 Publication Date

August 2020

## 5.2 Date Last Updated

November 2022